Aerosol and Air Quality Research

ORIGINAL RESEARCH
https://doi.org/10.4209/aaqr.210293

# $PM_{10}$ Source Identification: A Case of a Coastal City in Colombia

**Leandro Gómez-Plata[1*], Dayana Agudelo-Castañeda[2], Margarita Castillo[1], Elba C. Teixeira[3]**

[1] Department of Environmental Engineering, Corporation Universitario Reformada, Barranquilla, Colombia
[2] Department of Civil and Environmental Engineering, Universidad del Norte, Barranquilla, Colombia
[3] Postgraduate Program in Remote Sensing, Universidade Federal do Rio Grande do Sul, Porto Alegre, Brazil

## ABSTRACT

This paper assesses the spatial variation of EC, OC, major, and trace elements in an industrialized coastal city, allowing identification and tracers of $PM_{10}$ emission sources. 83 samples (24 h average) were collected on quartz filters during the dry season using high-volume samplers. Major and trace elements were analyzed using ICP-AES and ICP-MS, whereas a thermal/optical carbon analyzer was used to determine OC and EC. Chemical characterization of major elements, $SiO_2$, $SO_4^{2-}$, MgO, and CaO, showed high spatial variation between sites. The abundance of these major elements and OC confirmed the effect of exposed land resuspension and road dust; mutually with the production of secondary organic aerosol (SOA). Trace elements showed high values of Cu, Pb, Mn, and V, indicating the influence of road traffic and some industries (Cu) and oil burning (V and Mn). Enrichment Factor analysis revealed that Mg, P, S, Cu, and Pb were highly/moderately enriched indicating the substantial contribution of anthropogenic sources. Results of diagnostic ratios and PMF receptor model of the spatially obtained data suggested major sources of $PM_{10}$ as traffic-related emissions, heavy fuel oil combustion, biomass burning, and industrial processes. Back trajectory analysis (HYSPLIT) indicated air masses were coming from the North-East region of the Atlantic Ocean as the principal origin.

**Keywords:** $PM_{10}$, SPATIAL variation, PMF model, Enrichment factor, TRACE elements



**Received:** October 23, 2021
**Revised:** June 6, 2022
**Accepted:** July 14, 2022

* **Corresponding Author:**
lgomezplata@gmail.com

**Publisher:**
Taiwan Association for Aerosol Research
**ISSN:** 1680-8584 print
**ISSN:** 2071-1409 online



## 1 INTRODUCTION

Understanding atmospheric particles and chemical characterization is a continuing concern within public health, due to their possible adverse effects (Englert, 2004; Pey *et al.*, 2010a). Studies of particulate matter (PM) with aerodynamic diameter $< 10$ μm ($PM_{10}$) have become a major concern in developing countries related due to their association with morbidity and mortality, reduction in lung function, and exacerbation of airway illnesses (Agudelo-Castañeda *et al.*, 2019; Hsu *et al.*, 2016; Rodríguez-Villamizar *et al.*, 2019). For this purpose, positive matrix factorization (PMF) has become the most extensively used pollution source resolution method in research around the world (Gadi *et al.*, 2019; Jain *et al.*, 2020; Pant and Harrison, 2012; Sharma *et al.*, 2016, 2014; Shivani *et al.*, 2019). While EPA PMF (V5.0) incorporates considerably enhanced error estimation methods, which try to estimate the errors happening to the inherent uncertainties in the data and the rotational ambiguity in the result (Hopke, 2016; Paatero *et al.*, 2014). Moreover, the chemical composition of $PM_{10}$, especially trace metal content, has been widely used to infer $PM_{10}$ sources (Li *et al.*, 2021; Sharma *et al.*, 2014).

Although the importance of analyzing the global, regional, and local influences in this region,

studies in Caribbean urban coastal zones are scarce (Agudelo-Castañeda *et al.*, 2020; Aldabe *et al.*, 2011; Arruti *et al.*, 2011; Kalaiarasan *et al.*, 2016; Li *et al.*, 2021; Moreno *et al.*, 2010a; Police *et al.*, 2016) Because of their location and prevailing wind direction, the study area may receive a high influence from regional air masses, industrial sources, and traffic, causing high loading of trace elements. Even if these elements frequently account for a minor proportion of PM, they have substantial environmental and human health impacts (González-Castanedo *et al.*, 2014; Hao *et al.*, 2018; Minguillón *et al.*, 2014; Ripoll *et al.*, 2015). For instance, cadmium, cobalt, arsenic, chromium, nickel, and lead are considered human carcinogens (Liu *et al.*, 2018). Regardless of the importance of public health and risk, there is no baseline information concerning atmospheric pollutant emissions, dynamics, and principal sources of trace elements in the study area. Therefore, this study makes a major contribution to research on chemical element sources in $PM_{10}$ in a highly industrialized area.

The first section (i) of this paper assesses the spatial variation of OC, EC, EC, major, and trace elements of $PM_{10}$ in an industrialized Caribbean city. The next section (ii) focuses on the evaluation of $PM_{10}$ emission sources focusing on the Enrichment Factor and chemical characterization. The last section (iii) discusses PMF profiles and air masses trajectories to deduce the causes of PM peak pollution. Therefore, this work will provide one of the first investigations through spatially resolved data of trace elements associated with $PM_{10}$ that may be used for public health studies and fill the nonexistence of information in the region.

## 2 METHODS

### 2.1 Study Area

The study area is located on the western side of the river delta of the Magdalena River, and nearby the Caribbean Sea. Barranquilla is the central economic and industrial hub of the Colombian Caribbean Region with 1,193,952 inhabitants (Barranquilla, 2018). The average annual rainfall is 750.1 mm in 55 days with dry and wet seasons, where the principal dry season is December–April. Bimodal precipitation consists of two periods in May–June and August–November. In July, a reduction of precipitations is registered, although less pronounced than in January. The annual average relative humidity is 83% with 1652 mm of evapotranspiration. The dry season (December–March) is characterized by its lower relative humidity of 78%. In these dry months, the sun on average shines for 8–9 hours. The month with the lowest solar brightness is October with 6 hours $day^{-1}$. During the sampling period (March 17–April 4, 2016), weather conditions were like climatological normals, with small deviations. Ambient temperature, relative humidity, wind speed, and direction data were taken from two Mark Davis Vantage PRO 2 stations located in two sampling points: Pies Descalzos and Cotediba. The prevailing wind was NE and NW for Pies Descalzos and Cotediba, respectively. Following the Köppen climate classification, the climate in the study area is tropical wet and dry savanna Aw, characterized by an average annual temperature of 28°C, with an average annual minimum of 25.1°C and a maximum of 31.4°C (IDEAM, 2016). The prevailing wind was from the northeast (31.4%) all year, with the second predominance of winds from the north (29.9%). The annual occurrence of calm winds ($< 0.5$ m $s^{-1}$) was 9.7% with an annual average wind speed of 10–11 m $s^{-1}$ (IDEAM, 2016). Wind speed and relative humidity ranged between 5.7–8.8 m $s^{-1}$ and 77-87%, respectively, during the sampling period. Moreover, relative humidity decreased in the last week of March. The average ambient temperature was 28.6°C and 27°C for Pies Descalzos and Cotediba, respectively. Some industries use diesel fuel, while most use natural gas, supplementary information is included in SI1. The location of the sampling sites in the study may be observed in Table 1 and Fig. 1.

### 2.2 Sampling and Chemical Analysis

Simultaneous measurements of $PM_{10}$ (airborne particle matter $< 10$ μm) concentrations at seven sampling sites representing regional, urban, and industrial environments were carried out. Sampling was conducted by the Environmental Authority of Barranquilla and filters were kindly provided as part of a joint project.

Airborne particle matter $< 10$ μm ($PM_{10}$) was measured using high volume samplers (1.1–1.7 $m^3$ $min^{-1}$) Model TE 6070-MFC PM10, TISCH environmental brand (EPA approved Manual

**Table 1.** Location of sampling sites.

| Point | Site | N | W | Description |
|---|---|---|---|---|
| P1 | Portales de Sevilla | 11°1'0.95" | 74°48'50.09" | *Residential area, although is impacted by some chemical industrial sources, cement plant and harbors.* |
| P2 | Pies Descalzos | 11°1'43.71" | 74°52'5.91" | *Public school located near a quarry, the sea, and the river.* |
| P3 | Juan Mina | 10°57'21.50" | 74°53'36.01" | *The western´s point is in a region characterized by several hazardous waste incinerators and brickkilns.* |
| P4 | Inmaculada Concepción | 10°56'36.91" | 74°49'17.97" | *The southern point is in an area with several common industries and cemeteries.* |
| P5 | Cotediba | 10°57'1.27" | 74°46'58.39" | *It is in the south of the city, too, near several ports and common industries* |
| P6 | Barrio Abajo | 10°57'1.27" | 74°47'10.87" | *Residential area, although some chemical and food industries are near* |
| P7 | La Manga | 10°59'21.10" | 74°49'27.02" | *Residential area* |

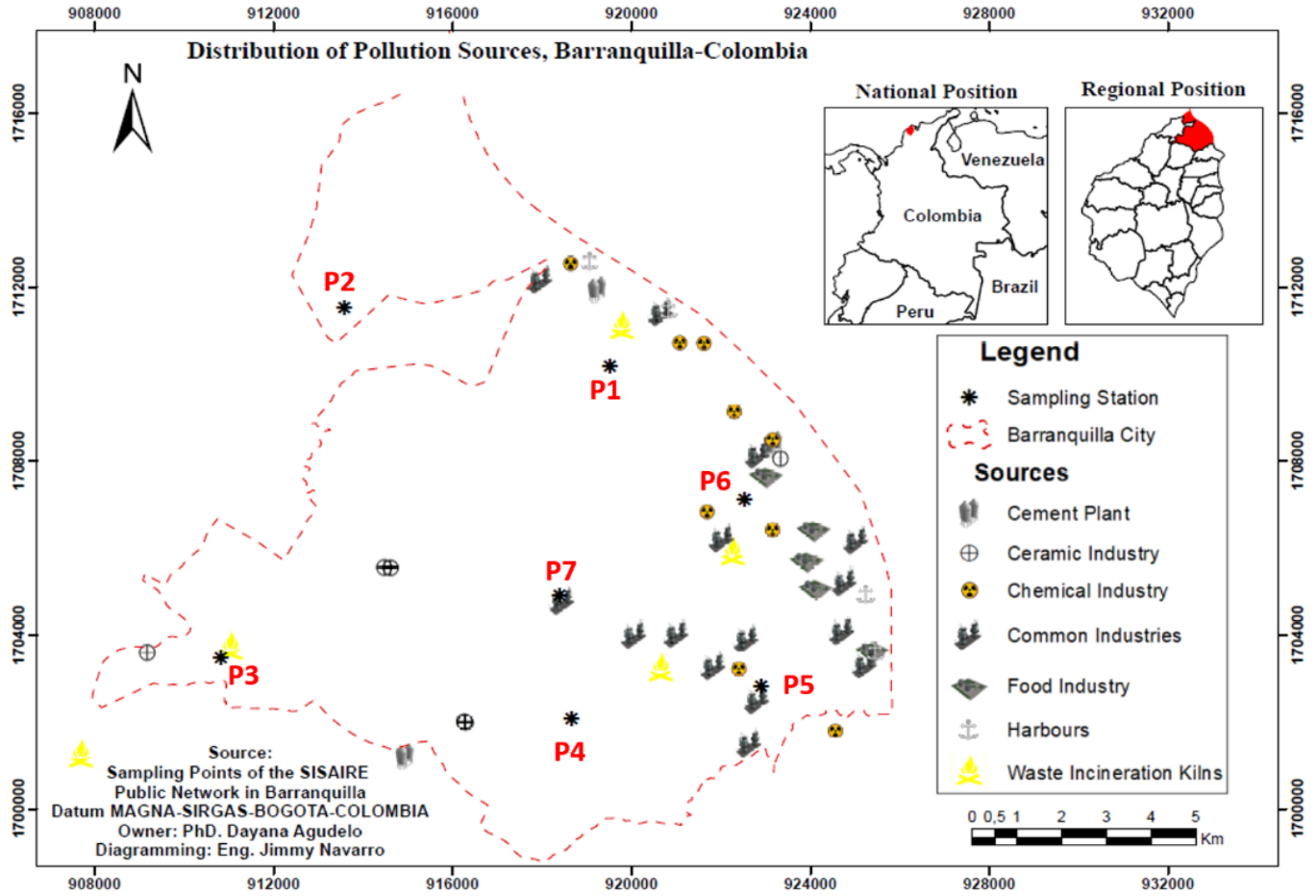


**Fig. 1.** Study area and sampling sites in Barranquilla.

Reference Method: RFPS-1287-063) (U.S. EPA, 1999). QA/QC was included in SI4 and SI5. The sampling period was 17 days (March 17–April 4, 2016), during the dry season. A total of 83 samples were obtained. Airborne particles were collected on ALBET quartz filters (203 × 254 mm) over a period of 24 hours ± hour. Particle mass concentrations were determined by standard gravimetric procedures (SI1). Each filter was weighed before and after sampling to determine the net weight of the collected $PM_{10}$ sample. More details may be consulted in SI1.

Filters were subjected to different treatments in acidic digestion ($HNO_3$:HF: $HClO_4$) of ½ of each filter; and an analysis of organic carbon (OC) and elemental carbon (EC) in 1.5 $cm^2$ sections. The

extracted solution from the acidic digestion was analyzed by Inductively Coupled Atomic Emission Spectrometry, ICP-AES, (IRIS Advantage TJA Solutions, THERMO) for the determination of the major elements, and Inductively Coupled Plasma Mass Spectrometry, ICP-MS, (X Series II, THERMO) for the trace elements. OC and EC were determined by a thermal/optical carbon analyzer (SUNSET), using protocol EUSAAR_2. Details of the procedure and chemical analysis are provided in the supplementary materials (SI1, SI2, SI4, SI5). Other analytical details may be found in Querol *et al.* (2009).

### 2.3 Positive Matrix Factorization (PMF)

Positive matrix factorization (PMF) is a multivariate factor analysis tool that partition the data into factor contributions, profiles, and a residual matrix (Brown *et al.*, 2015; Paatero, 1997; Paatero *et al.*, 2014). The fundamental principle of the model is mass conservation may be assumed and thus, a mass balance analysis can be used to detect and apportion sources of atmospheric particles (Hopke, 2016). We used the EPA PMF v5.0 (U.S. EPA, 2018). PMF methodology is explained, briefly in supplementary materials (SI1) and another published study (Agudelo-Castañeda and Teixeira, 2014; Teixeira *et al.*, 2015). The determination of factor profiles in PMF is an important process and depends on the goodness of fit to the original data (Agudelo-Castañeda and Teixeira, 2014). Consequently, six factors were used because they can be explained by known source patterns and physically realistic results. Major and trace elements were chosen based on the signal-to-noise ratio, the percentage of values above the MDL, and the database size requirements. Just 16 species were selected as strong, 29 were classified as bad and 11 were classified as weak. Weak species had their uncertainty magnified by a factor of 3, and bad species were eliminated. The model was run numerous times with a differing factors number (3–8) using random seed mode. Q theoretical value was very similar to the obtained Q in the model, thus representing an applicable uncertainty in the input. Scaled residuals values were in the recommended range (–3 to +3) (Comero *et al.*, 2009). Details of PMF settings, regression diagnostics, and Q values results are provided as supplementary materials (SI1, Table S1, S2, and S3).

### 2.4 Enrichment Factor (EF) Analysis

The enrichment factor (EF) is widely applied to identify the anthropogenic source of chemical elements (Hans Wedepohl, 1995). Calculation of the enrichment factor of each element detected in the study area was done using Ti as the reference element and composition of the upper continental (Fomba *et al.*, 2013; McLennan, 2001). Eq. (1) was applied for the calculation of the enrichment factor of each sampling site in the study area:

$$EF = \frac{\left(\frac{C_x}{C_R}\right)_{PM}}{\left(\frac{C_x}{C_R}\right)_{crust}} \quad (1)$$

where EF is the enrichment factor of element *x* that represents the chemical element of interest. $C_x$ *i*s the concentration of each element in the $PM_{10}$ sample, where $C_R$ is the concentration of the reference element in the upper continental crustal. $(C_x/C_R)_{PM}$ is the concentration ratio of element *x* to *R* element in the $PM_{10}$ sample and $(C_x/C_R)$Crust is the concentration ratio of *X* to *R* element in the crustal material.

## 3 RESULTS AND DISCUSSION

### 3.1 $PM_{10}$ and Major Chemical Species

Table 2 summarizes the average concentration of major elements, $PM_{10}$, OC, and EC ($\mu g\ m^{-3}$). Results evidenced high $PM_{10}$ levels (mean $51.7 \pm 10.5\ \mu g\ m^{-3}$), especially in P3 up to P7, the latter nearly 3-fold the WHO annual $PM_{10}$ guideline. Spatial variation (see Table 1 and Fig. 1 for the location of sampling sites) results indicated that P1 (Portales de Sevilla, a residential area) had

**Table 2.** The average concentration of major elements, $PM_{10}$, OC, and EC (μg $m^{-3}$).

| | Average | P1 Portales de Sevilla | P2 Pies Descalzos | P3 Juan Mina | P4 Inmaculada Concepción | P5 Cotediba | P6 Barrio Abajo | P7 La Manga |
|---|---|---|---|---|---|---|---|---|
| $PM_{10}$ | 51.7 ± 10.5 | 30.7 | 43.7 | 58.3 | 57.4 | 51.2 | 57.4 | 59.1 |
| $Al_2O_3$ | 2.01 ± 0.75 | 0.61 | 1.14 | 2.52 | 2.23 | 2.33 | 2.41 | 2.31 |
| $SiO_2$ | 5.02 ± 1.87 | 1.53 | 2.84 | 6.30 | 5.58 | 5.82 | 6.02 | 5.77 |
| CaO | 2.85 ± 1.17 | 0.70 | 1.65 | 3.21 | 2.93 | 3.48 | 4.18 | 2.93 |
| $Fe_2O_3$ | 0.82 ± 0.27 | 0.32 | 0.50 | 0.95 | 0.88 | 0.95 | 1.02 | 0.91 |
| $K_2O$ | 1.34 ± 0.24 | 0.98 | 1.08 | 1.51 | 1.59 | 1.53 | 1.25 | 1.42 |
| MgO | 5.19 ± 0.57 | 4.22 | 4.73 | 5.95 | 5.53 | 5.27 | 5.45 | 5.07 |
| $P_2O_5$ | 1.13 ± 0.49 | 1.44 | 1.13 | 0.54 | 1.52 | 1.62 | 0.48 | 1.61 |
| $TiO_2$ | 0.11 ± 0.04 | 0.05 | 0.07 | 0.12 | 0.12 | 0.13 | 0.14 | 0.12 |
| $SO_4^{2-}$ | 5.01 ± 1.29 | 2.91 | 3.47 | 6.16 | 6.37 | 4.75 | 4.87 | 5.42 |
| OC | 2.31 ± 0.50 | 1.60 | 1.71 | 2.64 | 2.98 | 2.50 | 2.29 | 2.14 |
| EC | 0.17 ± 0.06 | 0.08 | 0.09 | 0.18 | 0.22 | 0.20 | 0.19 | 0.18 |

the lowest levels for almost all major elements, except for $P_2O_5$. Probably, because of their location, upstream of primary emission sources (the predominant wind direction was NE for the meteorological station in P2). Additionally, the highest $PM_{10}$ concentrations were observed at the southernmost sampling sites: P6 (residential area) and P7 (residential area). Sampling site P3 is characterized by near quarries and exposed land, thus, the slightly higher $PM_{10}$ concentrations compared with the nearby sites. This pattern was observed for crustal elements, too that presented contributions of Al and Mg elements (Table 2). The sampling period corresponded to the dry season, where resuspension increases due to their dry climate. The soil of the study area is characterized by layers of sandy, marly, and loam limestones (limestone - clay - caliche), and coralline rocks, composed of Ca, Al, and Si (IGAC, 2017). Results showed, too, a high concentration for $SiO_2$, MgO, and CaO, though with a slight spatial variation between sites.

MgO was constant between sites, indicating the presence of limestone (dolomite). Moreover, $SiO_2$ and CaO levels were lower in P1 and P2. Probably, as explained above, because P1 and P2 location is upstream of main emission sources and may be considered "background" sites. MgO, $Al_2O_3$, and $SiO_2$ showed the highest concentrations in P3 due to the near quarries.

Cement industries and construction originated CaO high levels, i.e., P6 presented the highest concentrations for CaO, probably of some road construction works done nearby for a stream canalization.

The abundance of all these major elements confirms the effect of the resuspension of exposed land and road dust. The city, too, uses concrete pavement in mostly all the streets. This issue and the problem of inadequate rainwater sewerage system cause the deterioration of roads and possible production of dust that may be resuspended.

Furthermore, P4 (common industries and cemeteries) presented the highest concentrations for $SO_4$, OC, and EC. This site is downstream of diverse industries (the prevailing wind direction for P5 was NW), especially several brickkilns and hazardous waste incinerators. Brickkilns may use combustible sulfur which is a precursor of sulfated aerosols, thus increasing $SO_4$ concentrations and organic compounds.

A comparison of the findings with those of other studies confirms that the relatively high levels of K might indicate that biomass burning impact on $PM_{10}$ levels is high (Rolong *et al.*, 2021). Though, the high correlation K/Al ($R^2$ = 0.72) suggests that K is present in mineral matter. Also, results showed significant correlations between OC and K ($R^2$ = 0.64). The sum of mineral matter-related oxides accounts for the largest proportion of the $PM_{10}$ mass (30–32% P1–P2 and 34–41% P3–P7).

Fig. 2 presents the correlation between OC and EC in all sampling sites (a) and by site (b). Results showed significant correlations between OC and EC ($R^2$ = 0.77), although mostly all correlations were > 0.98 (Fig. 2(b)), except for the sampling site P3. These correlations and proportional relative rates of OC and EC emission to each other may indicate the presence of common dominant sources (Kong *et al.*, 2010). Even if the sampling sites were highly impacted by vehicles and industrial

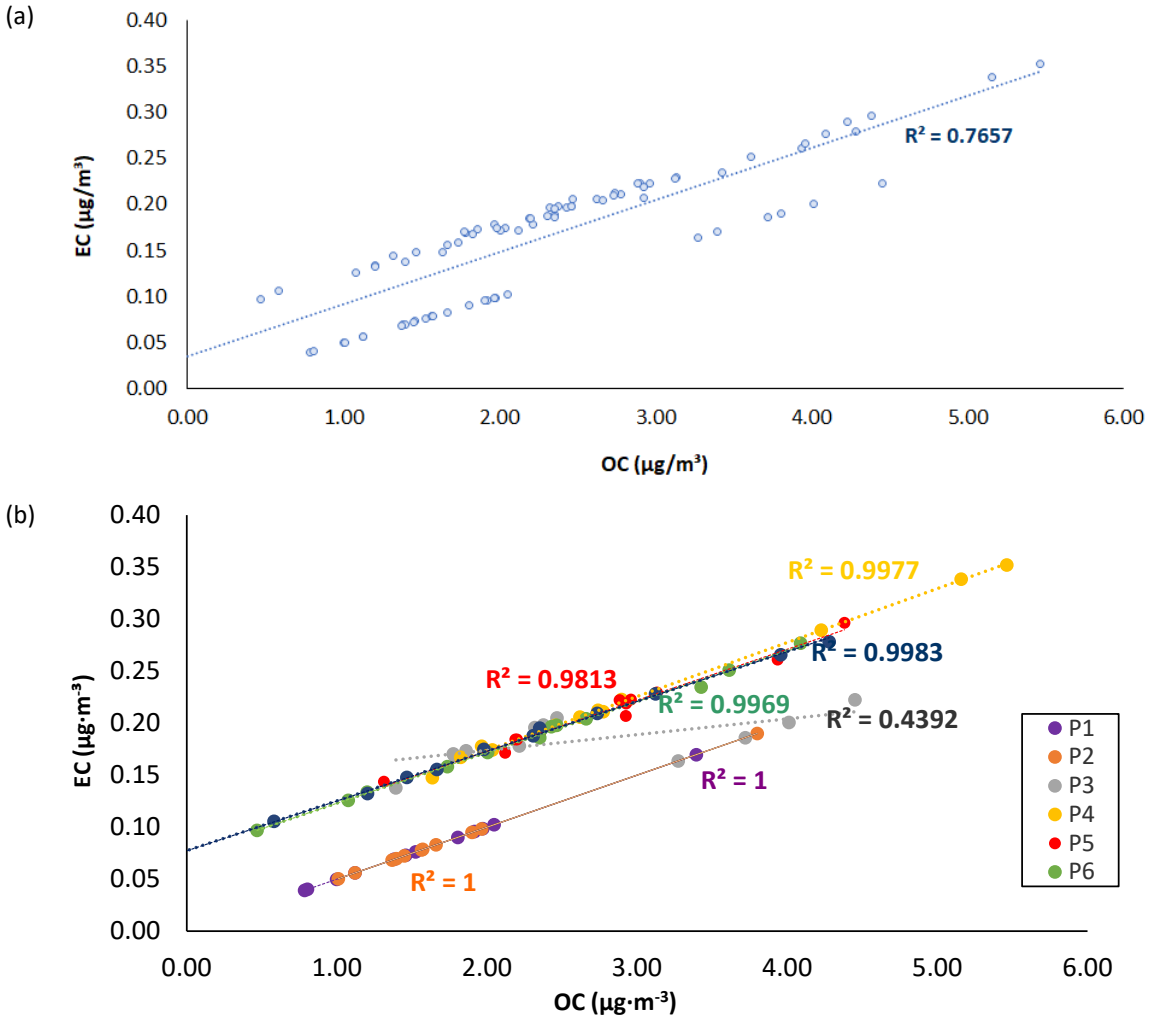


**Fig. 2.** Correlation between OC and EC in (a) all sampling sites and (b) by the site.

sources, levels of EC were low (1 order of magnitude lower than most European and Indian cities, Mahapatra *et al.*, 2021; Reche *et al.*, 2011), and as expected much lower than OC, with OC/EC ratios close to 20 for P1 and P2 (Fig. 2(b)) and 11–15 for P3–P7, possibly pointing to high production of secondary organic aerosol (SOA). P1 and P2 located the nearest to *Isla Salamanca Natural Park* on the northeastern side of the Magdalena River (Fig. 1) showed similar OC/EC ratios with high correlations values (Fig. 2(b)). This natural Park suffers along in the dry season from several fires caused by the high temperatures or by burning the mangrove wood for coal production, cattle raising, or farming. The Caribbean region is particularly vulnerable to fire occurrence due to large seasonal water deficits (Hoyos *et al.*, 2017). Thus, a high impact of biomass combustion and/or the influence of the dry climate, with high temperatures and relative humidity, the presence of hydric resources, and mangroves that favor SOA production, may account for these high OC/EC ratios. In the study area, roads are constructed with concrete, which requires higher energy use compared with an asphalt surface, which marks in higher fuel consumption hydrocarbon concentrations, resulting probably in high OC/EC values (Adamiec *et al.*, 2016). On the other hand, P3 showed the lowest correlation value ($R^2$ = 0.44). This site is an industrial site impacted by hazardous waste incinerators and brick kilns.

## 3.2 Enrichment Factor

Fig. 3 shows the mean Enrichment Factors (EF) for the seven sampling sites. Some trace elements, classified as toxic compounds by the International Agency for Research on Cancer (IARC, 2017) such as Ni (group 1: "Carcinogenic to humans") and Pb (group 2A: "Probably carcinogenic to

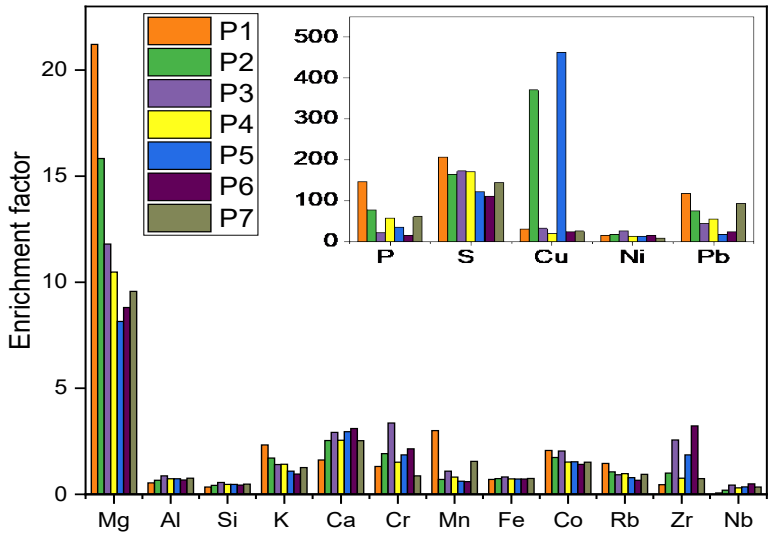


**Fig. 3.** Mean Enrichment Factors (EF) for the seven sampling sites.

humans"), showed moderately and high EF. EF crust close to one indicates the crust (resuspension of soil) as the likely source of the element. Al, Si, K, Ca, Mn, Cr and Fe showed this pattern, meaning probably crustal influence. Mg and Ni ($10 < EF < 50$) appeared to be moderately enriched, while P, S, and Cu ($EF > 100$) were highly enriched for some sites. High EF values for S were obtained for all sampling sites, indicating possible vehicular traffic emissions. In Colombian cities, before May 2021 vehicles use diesel with a sulfur content of 50 ppm (about 5.98% of all), while mostly all private and public cars use gasoline with 300 ppm, including motorcycles (ANDEMOS, 2018; ECOPETROL, 2018). Moreover, the economic growth of the city implied a rising demand for transportation, thus vehicle numbers increased by approximately 10.000 year$^{-1}$; whereas approximately 20% of additional cars circulate in Barranquilla with a license plate from another city. Closer inspection of both Ni and Cu EF values in Fig. 3 (moderately enriched) shows similar values for all sites (except for P2 and P5 for Cu EF values), thus, confirming the vehicular traffic influence. Probably, in P2 and P5 the presence of irregular smelter processes emitted these high concentrations. On the other hand, Fig. 3 reveals highly enriched EF values for Pb in P1, P2, and P7 sites. The two latter sites are characterized by irregular Pb smelters for artisanal recovery of this metal in old batteries, which were in operation at the time of sampling. Moreover, P1 and P7 high EF values are probably due to their location near the harbors, thus receiving a high influence on shipping emissions. Consequently, high EF values in the city probably are due to Pb in emissions of irregular smelters and harbors. Moderately enriched EF values of P, principally in P1, are probably due to a fertilizer industry located near the sampling site. Moreover, fossil fuel combustion is estimated to be a major source of atmospheric-P in industrialized regions (Weinberger *et al.*, 2016) besides the particle phase phosphorus emitted from biogenic processes (Rizzo *et al.*, 2010).

## 3.3 Tracer Species for Source Identification

Table 3 shows the average concentration of trace elements for all sampling sites. As explained above, high EF values of Cu, Pb, and Ni were obtained. Moreover, high concentrations of Cu, Pb, and V were measured. Vanadium is a tracer of the influence of oil-burning (all sites). The maximum Cu value obtained for all samples was 496.2 ng m$^{-3}$. Cu mean values reached near 117.5 and 323.1 ng m$^{-3}$ at P2 and P5, respectively, pointing to the influence of industrial emissions at these sites, such as smelter processes, besides road traffic (González-Castanedo *et al.*, 2014). These results may confirm the high EF values for these two sites (P2 and P5).

Pb reached sporadically near 340 ng m$^{-3}$ values, without major correlation with other trace elements out of As and Sn. Probably pointing to infrequent emissions of a high-temperature industrial process, principally in P1–P2 sites due to their proximity to the industries area near the harbors. As explained above, these two sites presented high EFs values, whereas P1 showed

**Table 3.** The average concentration of trace elements for all sampling sites (ng $m^{-3}$).

| | Average | SD | P1 Portales de Sevilla | P2 Pies Descalzos | P3 Juan Mina | P4 Inmaculada Concepción | P5 Cotediba | P6 Barrio Abajo | P7 La Manga |
|---|---|---|---|---|---|---|---|---|---|
| V | 8.59 | 3.03 | 4.35 | 5.25 | 10.88 | 11.66 | 11.66 | 7.27 | 9.05 |
| Cr | 2.33 | 1.38 | 0.67 | 1.49 | 4.40 | 2.07 | 3.18 | 3.45 | 1.04 |
| Mn | 18.88 | 7.64 | 23.32 | 8.21 | 21.53 | 16.76 | 15.83 | 14.40 | 32.13 |
| Co | 0.37 | 0.10 | 0.22 | 0.26 | 0.49 | 0.38 | 0.47 | 0.40 | 0.37 |
| Ni | 7.20 | 3.36 | 3.41 | 5.44 | 13.18 | 6.09 | 8.69 | 9.11 | 4.48 |
| Cu | 72.33 | 117.3 | 6.53 | 117.5 | 17.26 | 11.75 | 323.1 | 15.79 | 14.37 |
| Cd | 0.16 | 0.06 | 0.12 | 0.10 | 0.19 | 0.26 | 0.19 | 0.11 | 0.14 |
| Sn | 1.44 | 0.35 | 1.36 | 1.48 | 1.68 | 2.00 | 1.51 | 0.98 | 1.07 |
| La | 1.01 | 0.21 | 0.65 | 0.79 | 1.18 | 1.13 | 1.18 | 1.09 | 1.08 |
| Ce | 1.82 | 0.43 | 1.12 | 1.39 | 2.15 | 1.85 | 2.17 | 2.28 | 1.79 |
| Pb | 23.95 | 11.31 | 24.85 | 23.36 | 21.01 | 27.89 | 10.83 | 14.02 | 45.65 |
| As | 0.64 | 0.12 | 0.54 | 0.56 | 0.63 | 0.84 | 0.74 | 0.50 | 0.69 |

high values for P, S, and Pb (Table 2 and Table 3), and P2 for the same elements plus Cu. These sporadic Pb and Cu concentrations associated with $PM_{10}$ may indicate the influence of industrial processes and shipping emissions (Nunes *et al.*, 2017; Russo *et al.*, 2018; Viana *et al.*, 2014b). Ni had similar concentrations in all sites, confirming the influence of vehicular traffic, except for P3. These results can be attributed to industry emissions such as cement and brick production (Taghvaee *et al.*, 2018).

Table 4 shows our results compared to previous studies. Fe concentration is less than that reported for the other cities, as well as the average concentration of Cr, which is lower than that reported for megacities in Latin America such as Mexico City and Bogotá. While Cr, Co, and Cd are close to those reported for other coastal cities in the Caribbean such as Belén, Costa Rica, and Cienfuegos, Cuba. Ni concentration is higher than that reported in other coastal cities, such as Navi, India, and Patras, Greece, and close to the reported concentration for Barcelona, Spain. Pb concentration is higher than that reported for all the cities in Table 4, except for Mexico and Barcelona.

The direct identification of anthropogenic emissions employing just these tracers is difficult because they are markers for many types of combustion processes occurring at the same time, such as industrial processes, traffic, petroleum refinery, and energy generation. Consequently, to better understand these values, some tracer species ratios were calculated for each sampling site (These results are like related studies in other cities -Tables 4 and 5-). Values confirmed the presence of different anthropogenic sources (Table 5). Cu/Pb ratio indicated traffic as a local source in P6 and P1 (Pey *et al.*, 2010a). Moreover, Cr/Pb ratio confirmed traffic as a source in P6 and P7 (Font *et al.*, 2015), while the Sb/Cu ratio fell in the range of traffic for P2, P5, and P6 (Pey *et al.*, 2010a). Sn/Cu ratio, confirmed too, the traffic influence in P2 and P5 sites, where values fall in the range for wear-abrasive sources (Lin *et al.*, 2015). The influence of shipping emissions was confirmed in all sampling sites as combustion processes that use crude oil as the main fuel, where vanadium (V) and nickel (Ni) are commonly identified as markers of shipping emissions (Viana *et al.*, 2014a). The study area is downwind of the prevailing wind direction, thus receiving shipping emissions, confirming the V/Ni and La/Ce ratios values for this type of local source originated in the North and Northeastern side of the city. These two latter ratios correlated very well with shipping emissions, as much of the combustion from ships derives V and Ni associated principally with fine atmospheric particles, and therefore capable of traveling long distances and staying resuspended (Viana *et al.*, 2014a). Moreover, the trace element ratio V/Co can be assigned to oil combustion according to literature (Ledoux *et al.*, 2017) for P1, P2, and P3 sites. Furthermore, the Mn/V ratio could be useful for distinguishing between particles originating from oil burning or coal-burning; while from oil burning this ratio is $<< 1$, from coal-burning, is $>> 1$ (Kong *et al.*, 2011). Ratios ranged from 1.36 to 5.36 which meant that $PM_{10}$ was more relative to heavy fuel oil combustion than coal burning in all sampling sites, probably originating from shipping emissions

**Table 4.** Comparison of the concentrations of PM and trace elements obtained in this study with other investigations.

| | This Study | Bogota, Colombia* | Belén, Costa Rica | Patras, Greece* | Cienfuegos, Cuba | Mexico City, Mexico | Barcelona, Spain | Navi Mumb, India | Delhi, India |
|---|---|---|---|---|---|---|---|---|---|
| $PM_{10}$ ($\mu g\ m^{-3}$) | 51.7 | 52.40 | 52 | 26.1 | 35.4 | 95 | 119.10 | 71 | 238 |
| Fe ($ng\ m^{-3}$) | 290 | 570 | 555 | 3480 | 540 | 3300 | 890 | 1900 | 7410 |
| V | 8.59 | 10 | - | -- | 11.34 | 30 | 13 | 7.2 | - |
| Cr | 2.33 | 30 | - | 0.9 | 2.99 | 70 | 6.0 | 26 | 320 |
| Mn | 18.88 | 20 | 140 | 9.3 | 11.11 | 60 | 2.4 | 41 | 260 |
| Co | 0.37 | - | - | 1.5 | 0.37 | - | - | - | - |
| Ni | 7.20 | 0.00 | 10 | 4.6 | 4.77 | 50 | 7.0 | 2.3 | - |
| Cu | 72.33 | 20 | 150 | 8.1 | 69.4 | 180 | 74 | 19 | 780 |
| Cd | 0.16 | - | - | -- | 0.15 | - | - | | - |
| Sn | 1.44 | - | - | -- | 0.41 | - | - | | - |
| Pb | 23.95 | 20 | 10 | 6.9 | 4.32 | 330 | 149 | 24 | 580 |
| As | 0.64 | - | - | -- | --- | - | - | | 150 |
| | | Industrial | Industrial | Urban | Urban | Urban | Urban | Urban | Urban |
| | ---- | Ramírez *et al.* (2018) | Murillo *et al.* (2013) | Manousakas *et al.* (2018) | Morera-Gómez *et al.* (2018) | Mugica *et al.* (2009) | Querol *et al.* (2001) | Police *et al.* (2016) | Jain *et al.* (2020) |

* Dry season.

**Table 5.** Average metal value ratios.

| Ratio | Portales de Sevilla | Pies Descalzos | Juan Mina | Inmaculada Concepción | Cotediba | Barrio Abajo | La Manga |
|---|---|---|---|---|---|---|---|
| | P1 | P2 | P3 | P4 | P5 | P6 | P7 |
| Cu/Cd | 451.0 | 53.77 | 1170 | 92.17 | 44.35 | 1691 | 139.8 |
| Cu/Pb | 0.263 | 5.031 | 0.822 | 0.421 | 29.82 | 1.126 | 0.315 |
| Cr/Pb | 0.097 | 0.027 | 0.064 | 0.209 | 0.074 | 0.293 | 0.246 |
| Sb/Cu | 0.020 | 0.122 | 0.006 | 0.141 | 0.225 | 0.005 | 0.042 |
| V/Ni | 75.79 | 22.40 | 40.09 | 34.10 | 31.58 | 33.84 | 77.87 |
| La/Ce | 0.556 | 0.577 | 0.567 | 0.549 | 0.608 | 0.543 | 0.479 |
| V/Co | 20.07 | 19.85 | 22.03 | 30.75 | 24.58 | 18.20 | 24.46 |
| Mn/V | 5.357 | 1.563 | 1.979 | 1.438 | 1.358 | 1.981 | 3.550 |
| Sn/Cu | 0.020 | 0.207 | 0.013 | 0.097 | 0.170 | 0.005 | 0.062 |

as stated above. Also, these sites may be impacted by possible recoveries of industrial oil. Ratio Cu/Pb and Cr/Pb confirmed the presence of municipal waste incinerators in P3 (Font *et al.*, 2015), where these ratios may be used as tracers. Slightly high Cu/Cd ratios in the study area confirmed the presence of additional emission sources of Cu from some industries, although, at some sampling points, these ratios were lower indicating the presence of close Cd sources, whereas Cu had also been recognized as markers for non-ferrous metal smelters (Kong *et al.*, 2011).

## 3.4 PMF Profiles

Profiles obtained from the PMF model identified six sources for $PM_{10}$. Results may be observed in Fig. 4. The identified sources were enriched road dust resuspension, biomass burning, traffic-related emissions, heavy fuel oil combustion, industrial/smelter processes, and brick.

Factor 1 was defined as enriched road dust resuspension with soil mineral dust because of their high loadings of crustal elements enriched in OC, EC, V, and Cd, among others. Possible sources may include emissions from near quarries located within the study area, besides resuspension of road dust (Amato *et al.*, 2009).

Factor 2 presented $P_2O_5$, MgO, and $K_2O$ with dominant concentrations. K is used as a key element for biomass burning or wood combustion (Sharma *et al.*, 2014). As explained before, a significant correlation between OC and K might give evidence of biomass burning as a source

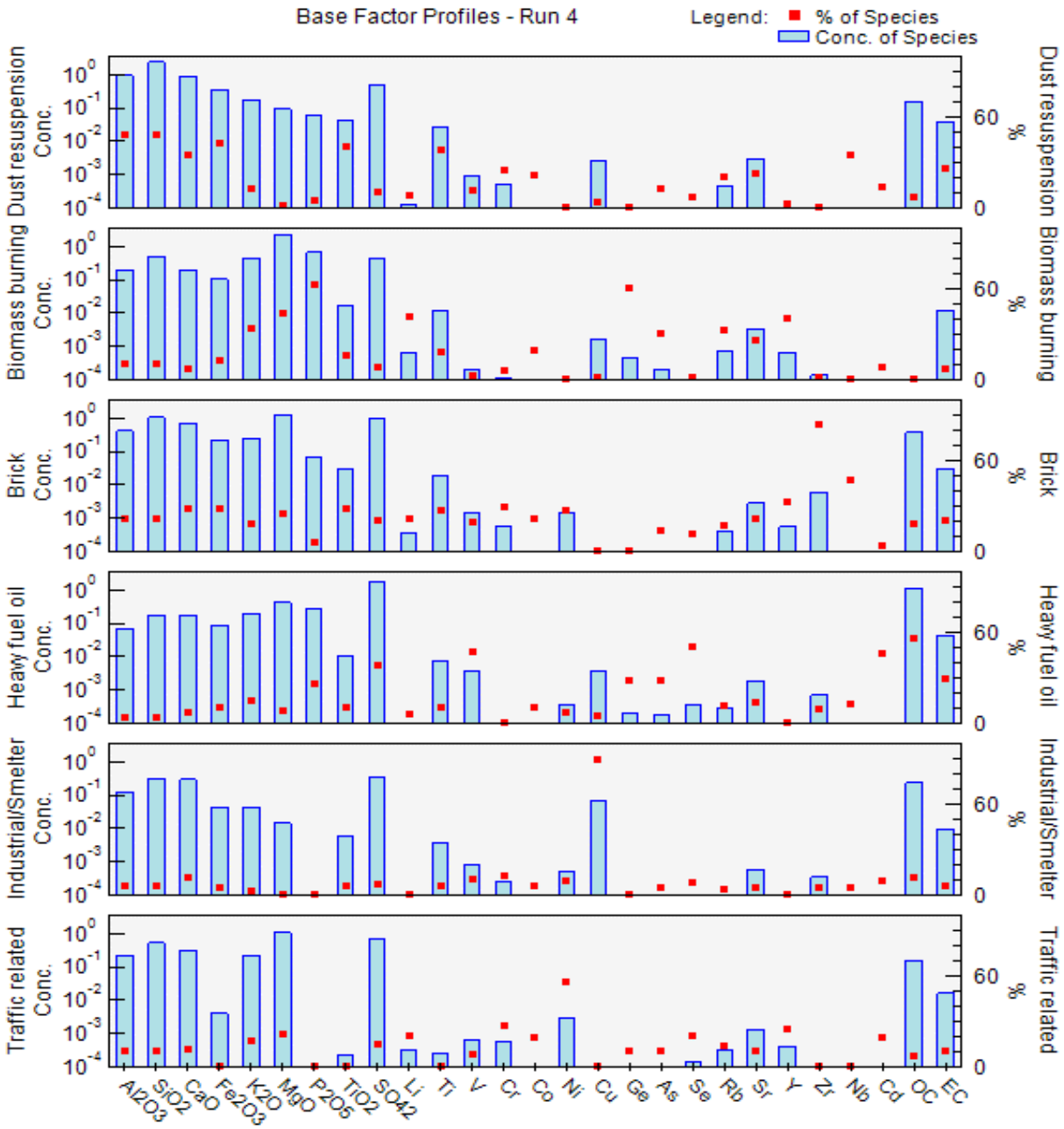


**Fig. 4.** Source profiles of PMF receptor model for $PM_{10}$ during the sampling period.

of $PM_{10}$ during the sampling period, which probably originated in the Isla Salamanca Natural Park on the northeastern side of the Magdalena River (Rolong *et al.*, 2021).

Factor 3 accounts for crustal elements and Zr with dominant concentrations. Zr was identified as a tracer of the ceramic industry, clay or clinker loading/transport (Minguillón *et al.*, 2013; Pey *et al.*, 2009; Sánchez de la Campa *et al.*, 2010). Several brickfields/ceramic industries that use coal or wood as main fuels have grown on the southwest side of the city near the P3 site. Consequently, this profile was defined as bricks/ceramics (Begum *et al.*, 2011).

Factor 4 had high loadings of V, Cd, OC, EC, and $SO_4^{2-}$. An increasing number of studies are showing that these elements are typical of heavy fuel oil combustion, probably originating from shipping emissions (Moreno *et al.*, 2010b; Pey *et al.*, 2010b; Viana *et al.*, 2014b), as explained above.

Factor 5 was identified as industrial and smelter processes because presented high loadings of Cu. As explained above, Cu concentrations were high in some industrial sites, thus confirming

this result. Several studies state Cu is a tracer of non-ferrous smelters (Pan *et al.*, 2015) or even Cu-smelter processes (González-Castanedo *et al.*, 2014).

Factor 6 presented high values for Ni, Cr, Cd, EC, and $SO_4^{2-}$. These metals have been observed in other studies in the coarse fraction of atmospheric particle matter in high-traffic urban areas (Fomba *et al.*, 2018). Road dust resuspension generated by abrasion of vehicle parts and pavements may originate from these elements (Salvador *et al.*, 2012). Consequently, this profile was designed as traffic-related. As explained previously, the economic growth of the study area increased vehicle traffic and number.

### 3.5 Back Trajectory Analysis

HYSPLIT trajectories may be used to determine possible source regions contributing to air pollution in the study area or to determine air masses that may be affecting (Draxler *et al.*, 2020; Rolph *et al.*, 2017). All masses trajectories are in the supplementary information (SI3). $PM_{10}$ may travel long distances and stay suspended in air (Sharma *et al.*, 2014), thus 7 days were selected to calculate backward trajectories using HYSPLIT to understand the flow of pollutants from distant source regions. AGL heights of 500 m, 1000 m, and 1500 m were used to reduce the effects of surface friction (500 m) and to understand the behavior of the boundary layer. May be observed three different air masses trajectories during the sampling period (Fig. 5): one coming from the Northeast Atlantic Ocean and entering the northern region of Colombia, another one coming from east South America and crossing Venezuela, and the last one coming from the Caribbean Ocean and going through Venezuela. Recent studies demonstrate the possible influence of biomass burning in the Orinoquia region, thus increasing $PM_{10}$ (Ballesteros-González *et al.*, 2020).

This study has been of great importance for the environmental authority, since it has allowed us to recognize which are the main emitting sources of these trace metals, strengthening the management of air quality through the development of surveillance and control strategies, such as preparing the air quality management plan that contains programs and projects to reduce atmospheric pollution and trace metal level in Barranquilla, as well as the control of industries that impact air quality in the city. Our study suggests that to further reduce trace metal levels, we must encourage sustainable transport.

## 4 CONCLUSIONS

This paper assesses the spatial variation of chemical characterization of $PM_{10}$ in an industrialized Caribbean city and evaluation of emission sources using PMF, EF, and diagnostic ratios. As it is the first research in the study area, obtained results explained the origin of diverse trace elements associated with $PM_{10}$.

The results of this research support the idea of the contribution of *resuspension* of exposed land and road dust contribution to the study area.

Sites near *brickkilns and hazardous waste incinerators* contributed as precursors of sulfated aerosols.

Good correlations were found between OC and EC. Even if the sampling sites are highly impacted by vehicles and industrial sources, levels of EC were low, and as expected much lower than OC, possibly pointing to high production of secondary organic aerosol (*SOA*).

The impact of *biomass burning* was demonstrated, too.

High EF values for S were obtained for all sampling sites, indicating possible vehicular traffic emissions. Closer inspection of both Ni and Cu EF, and high EF values for S show similar values for all sites (except for P2 and P5 for Cu EF values), thus, confirming the *vehicular traffic* influence. Diagnostic ratios confirmed these results, which is the influence of traffic in the study area.

The influence of *shipping emissions* was confirmed in all sampling sites as combustion processes that use crude oil as the main fuel, where vanadium (V) and nickel (Ni) are commonly identified as markers; and high EF Pb values in P1 and P7 probably due to their location near the harbors. Also, the markers V and Ni pointed out the influence of heavy fuel oil combustion by the shipping emissions, too.

Cu mean values at P2 and P5 showed the influence of *industrial* emissions, such as smelter processes.

https://doi.org/10.4209/aaqr.210293

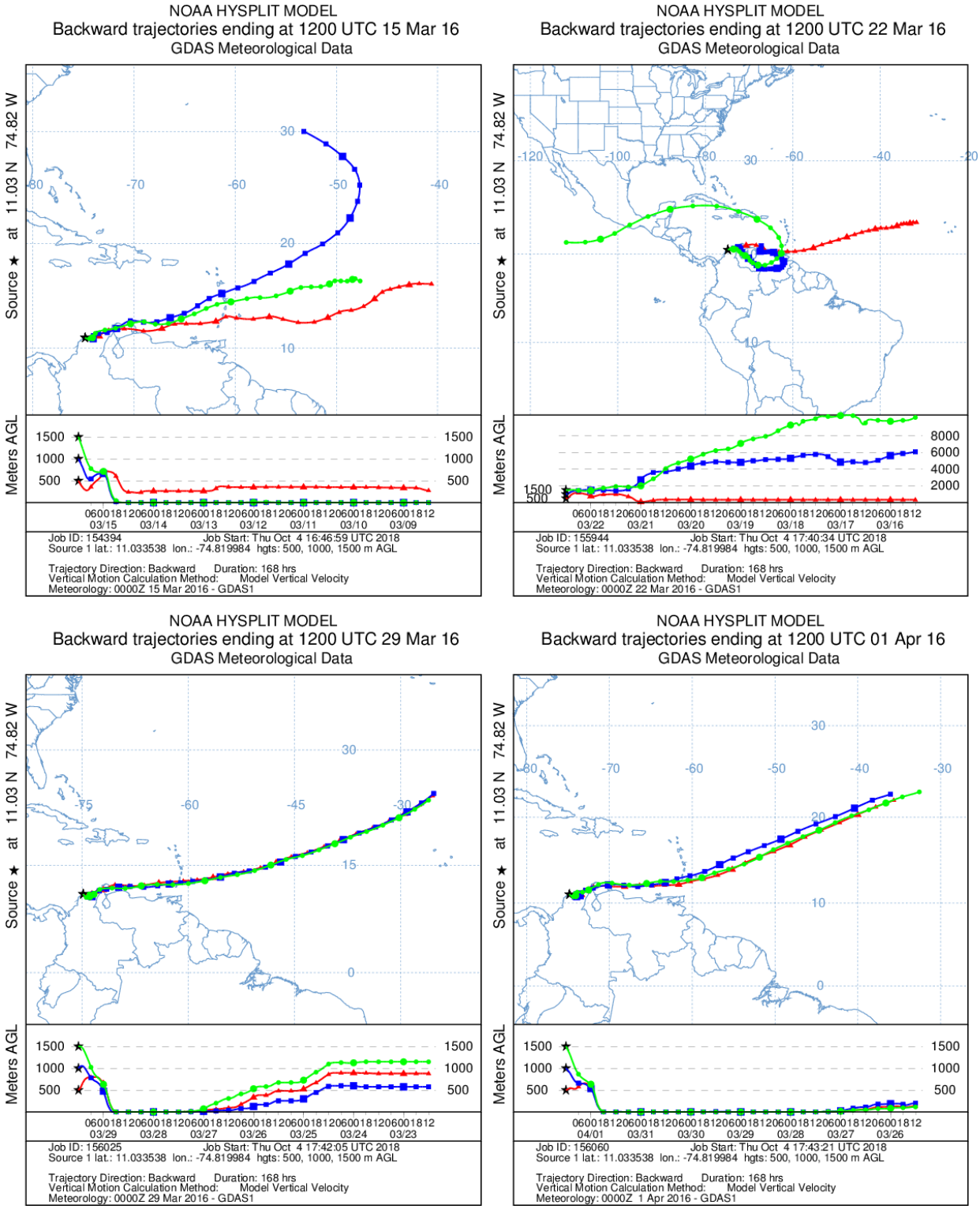


**Fig. 5.** Results of backward trajectory analysis.

PMF analysis confirmed some identified *sources* by ratios and EF values: enriched road dust resuspension, biomass burning, traffic-related emissions, heavy fuel oil combustion, industrial/ smelter processes, and brick.

These results could improve emission inventories and air quality management, overcoming the existing lack of information. The presented results show important implications regarding the scientific and environmental panorama.

## ACKNOWLEDGMENTS

The Environmental Agency of the District of Barranquilla - DAMAB (Actual EPA- Barranquilla Verde) and the Regional Environmental Agency (CRA – Atlántico) donated the $PM_{10}$ filters. To the Universidad de la Costa for the economic support for this research. The opinions, findings, ideas, and conclusions expressed in this publication are personal responsibility and do not commit to the Universidad del Norte or those of the supporting agencies.

## DISCLAIMER

Reference to any companies or specific commercial products does not constitute an endorsement, recommendation, or favoring of any university that participated in this research.

## SUPPLEMENTARY MATERIAL

Supplementary material for this article can be found in the online version at https://doi.org/10.4209/aaqr.210293

## REFERENCES

Adamiec, E., Jarosz-Krzemińska, E., Wieszała, R. (2016). Heavy metals from non-exhaust vehicle emissions in urban and motorway road dusts. Environ. Monit. Assess. 188, 1–11. https://doi.org/10.1007/s10661-016-5377-1

Agudelo-Castañeda, D.M., Teixeira, E.C. (2014). Seasonal changes, identification and source apportionment of PAH in $PM_{1.0}$. Atmos. Environ. 96, 186–200. https://doi.org/10.1016/j.atmosenv.2014.07.030

Agudelo-Castañeda, D., Calesso Teixeira, E., Alves, L., Fernández-Niño, J.A., Rodríguez-Villamizar, L.A. (2019). Monthly-Term Associations Between Air Pollutants and Respiratory Morbidity in South Brazil 2013-2016: A Multi-City, Time-Series Analysis. Int. J. Environ. Res. Public Health 16, 1–13. https://doi.org/10.3390/ijerph16203787

Agudelo-Castañeda, D., De Paoli, F., Morgado-Gamero, W.B., Mendoza, M., Parody, A., Maturana, A.Y., Teixeira, E.C. (2020). Assessment of the $NO_2$ distribution and relationship with traffic load in the Caribbean coastal city. Sci. Total Environ. 720, 137675. https://doi.org/10.1016/j.scitotenv.2020.137675

Aldabe, J., Elustondo, D., Santamaría, C., Lasheras, E., Pandolfi, M., Alastuey, A., Querol, X., Santamaría, J.M. (2011). Chemical characterisation and source apportionment of $PM_{2.5}$ and $PM_{10}$ at rural, urban and traffic sites in Navarra (North of Spain). Atmos. Res. 102, 191–205. https://doi.org/10.1016/j.atmosres.2011.07.003

Amato, F., Pandolfi, M., Escrig, A., Querol, X., Alastuey, A., Pey, J., Perez, N., Hopke, P.K. (2009). Quantifying road dust resuspension in urban environment by Multilinear Engine: A comparison with PMF2. Atmos. Environ. 43, 2770–2780. https://doi.org/10.1016/j.atmosenv.2009.02.039

Asociacion Nacional de Movilidad Sostenible (ANDEMOS) (2018). Asociación colombiana de vehículos automotores. http://www.andemos.org/ (accessed 31 July 2018).

Arruti, A., Fernández-Olmo, I., Irabien, A. (2011). Regional evaluation of particulate matter composition in an Atlantic coastal area (Cantabria region, northern Spain): Spatial variations in different urban and rural environments. Atmos. Res. 101, 280–293. https://doi.org/10.1016/j.atmosres.2011.03.001

Ballesteros-González, K., Sullivan, A.P., Morales-Betancourt, R. (2020). Estimating the air quality and health impacts of biomass burning in northern South America using a chemical transport model. Sci. Total Environ. 739, 139755. https://doi.org/10.1016/j.scitotenv.2020.139755

Barranquilla (2018). Alcaldía de Barranquilla. http://www.barranquilla.gov.co/index.php?option=com_content&view=article&id=27&Itemid=118 (accessed 31 July 2018).

Begum, B.A., Biswas, S.K., Hopke, P.K. (2011). Key issues in controlling air pollutants in Dhaka, Bangladesh. Atmos. Environ. 45, 7705–7713. https://doi.org/10.1016/j.atmosenv.2010.10.022

Brown, S.G., Eberly, S., Paatero, P., Norris, G.A. (2015). Methods for estimating uncertainty in PMF solutions: Examples with ambient air and water quality data and guidance on reporting PMF results. Sci. Total Environ. 518–519, 626–635. https://doi.org/10.1016/j.scitotenv.2015.01.022

Comero, S., Capitani, L., Gawlik, B.M. (2009). Positive Matrix Factorisation (PMF) - An introductioin to the chemometric evaluation of environmental monitoring data using PMF. Publications Office of the European Union, LU. https://doi.org/10.2788/2497

Draxler, R., Stunder, B., Rolph, G., Stein, A., Taylor, A. (2020). HYSPLIT User's Guide Version 5. Air Resources Laboratory, National Oceanic and Atmospheric Administration,USA.

ECOPETROL (2018). https://www.ecopetrol.com.co/wps/portal/es (accessed 31 July 2018).

Englert, N. (2004). Fine particles and human health - A review of epidemiological studies. Toxicol. Lett. 149, 235–242. https://doi.org/10.1016/j.toxlet.2003.12.035

Fomba, K.W., Müller, K., Van Pinxteren, D., Herrmann, H. (2013). Aerosol size-resolved trace metal composition in remote northern tropical atlantic marine environment: Case study cape verde islands. Atmos. Chem. Phys. 13, 4801–4814. https://doi.org/10.5194/acp-13-4801-2013

Fomba, K.W., van Pinxteren, D., Müller, K., Spindler, G., Herrmann, H. (2018). Assessment of trace metal levels in size-resolved particulate matter in the area of Leipzig. Atmos. Environ. 176, 60–70. https://doi.org/10.1016/j.atmosenv.2017.12.024

Font, A., de Hoogh, K., Leal-Sanchez, M., Ashworth, D.C., Brown, R.J.C., Hansell, A.L., Fuller, G.W. (2015). Using metal ratios to detect emissions from municipal waste incinerators in ambient air pollution data. Atmos. Environ. 113, 177–186. https://doi.org/10.1016/j.atmosenv.2015.05.002

Gadi, R., Shivani, Sharma, S.K., Mandal, T.K. (2019). Source apportionment and health risk assessment of organic constituents in fine ambient aerosols ($PM_{2.5}$): A complete year study over National Capital Region of India. Chemosphere 221, 583–596. https://doi.org/10.1016/j.chemosphere.2019.01.067

González-Castanedo, Y., Moreno, T., Fernández-Camacho, R., Sánchez de la Campa, A.M., Alastuey, A., Querol, X., de la Rosa, J. (2014). Size distribution and chemical composition of particulate matter stack emissions in and around a copper smelter. Atmos. Environ. 98, 271–282. https://doi.org/10.1016/j.atmosenv.2014.08.057

Hans Wedepohl, K. (1995). The composition of the continental crust. Geochim. Cosmochim. Acta 59, 1217–1232. https://doi.org/10.1016/0016-7037(95)00038-2

Hao, Y., Meng, X., Yu, X., Lei, M., Li, W., Shi, F., Yang, W., Zhang, S., Xie, S. (2018). Characteristics of trace elements in $PM_{2.5}$ and $PM_{10}$ of Chifeng, northeast China: Insights into spatiotemporal variations and sources. Atmos. Res. 213, 550–561. https://doi.org/10.1016/j.atmosres.2018.07.006

Hopke, P.K. (2016). Review of receptor modeling methods for source apportionment. J. Air Waste Manag. Assoc. 66, 237–259. https://doi.org/10.1080/10962247.2016.1140693

Hoyos, N., Correa-Metrio, A., Sisa, A., Ramos-Fabiel, M.A., Espinosa, J.M., Restrepo, J.C., Escobar, J. (2017). The environmental envelope of fires in the Colombian Caribbean. Appl. Geogr. 84, 42–54. https://doi.org/10.1016/j.apgeog.2017.05.001

Hsu, C.Y., Chiang, H.C., Lin, S.L., Chen, M.J., Lin, T.Y., Chen, Y.C. (2016). Elemental characterization and source apportionment of $PM_{10}$ and $PM_{2.5}$ in the western coastal area of central Taiwan. Sci. Total Environ. 541, 1139–1150. https://doi.org/10.1016/j.scitotenv.2015.09.122

International Agency for Research on Cancer (IARC) (2017). International Agency for Research on Cancer (IARC) Monographs on the Evaluation of Carcinogenic Risks to Humans - Agents Classified by the IARC Monographs, Volumes 1–117. http://monographs.iarc.fr/ENG/Classification/index.%0Aphp

Instituto Geográfico Agustín Codazzi (IGAC) (2017). http://geoportal.igac.gov.co:8888/siga_sig/Agrologia.seam (accessed 31 July 2018).

Jain, S., Sharma, S.K., Vijayan, N., Mandal, T.K. (2020). Seasonal characteristics of aerosols ($PM_{2.5}$ and $PM_{10}$) and their source apportionment using PMF: A four year study over Delhi, India. Environ. Pollut. 262, 114337. https://doi.org/10.1016/j.envpol.2020.114337

Kalaiarasan, G., Balakrishnan, R.M., Khaparde, V.V (2016). Receptor model based source apportionment of $PM_{10}$ in the metropolitan and industrialized areas of Mangalore. Environ. Technol. Innov. 6, 195–203. https://doi.org/10.1016/j.eti.2016.10.002

Kong, S., Han, B., Bai, Z., Chen, L., Shi, J., Xu, Z. (2010). Receptor modeling of $PM_{2.5}$, $PM_{10}$ and TSP in different seasons and long-range transport analysis at a coastal site of Tianjin, China. Sci. Total Environ. 408, 4681–94. https://doi.org/10.1016/j.scitotenv.2010.06.005

Kong, S., Ji, Y., Lu, B., Chen, L., Han, B., Li, Z., Bai, Z. (2011). Characterization of $PM_{10}$ source profiles for fugitive dust in Fushun-a city famous for coal. Atmos. Environ. 45, 5351–5365. https://doi.org/10.1016/j.atmosenv.2011.06.050

Ledoux, F., Kfoury, A., Delmaire, G., Roussel, G., El Zein, A., Courcot, D. (2017). Contributions of local and regional anthropogenic sources of metals in $PM_{2.5}$ at an urban site in northern France. Chemosphere 181, 713–724. https://doi.org/10.1016/j.chemosphere.2017.04.128

Li, J., Michalski, G., Olson, E.J., Welp, L.R., Larrea Valdivia, A.E., Larico, J.R., Zapata, F.A., Paredes, L.M. (2021). Geochemical characterization and heavy metal sources in $PM_{10}$ in arequipa, peru. Atmosphere 12, 1–14. https://doi.org/10.3390/atmos12050640

Lin, Y.C., Tsai, C.J., Wu, Y.C., Zhang, R., Chi, K.H., Huang, Y.T., Lin, S.H., Hsu, S.C. (2015). Characteristics of trace metals in traffic-derived particles in Hsuehshan Tunnel, Taiwan: Size distribution, potential source, and fingerprinting metal ratio. Atmos. Chem. Phys. 15, 4117–4130. https://doi.org/10.5194/acp-15-4117-2015

Liu, J., Chen, Y., Chao, S., Cao, H., Zhang, A., Yang, Y. (2018). Emission control priority of $PM_{2.5}$-bound heavy metals in different seasons: A comprehensive analysis from health risk perspective. Sci. Total Environ. 644, 20–30. https://doi.org/10.1016/j.scitotenv.2018.06.226

Mahapatra, P.S., Panda, U., Mallik, C., Boopathy, R., Jain, S., Sharma, S.K., Mandal, T.K., Senapati, S., Satpathy, P., Panda, S., Das, T. (2021). Chemical, microstructural, and biological characterization of wintertime $PM_{2.5}$ during a land campaign study in a coastal city of eastern India. Atmos. Pollut. Res. 12, 101164. https://doi.org/10.1016/j.apr.2021.101164

Manousakas, M., Diapouli, E., Papaefthymiou, H., Kantarelou, V., Zarkadas, C., Kalogridis, A., Karydas, A., Eleftheriadis, K. (2018). XRF characterization and source apportionment of $PM_{10}$ samples collected in a coastal city. X-Ray Spectrom. 47, 190–200. https://doi.org/10.1002/xrs.2817

McLennan, S.M. (2001). Relationships between the trace element composition of sedimentary rocks and upper continental crust. Geochem. Geophys. Geosyst. 2, 1021. https://doi.org/10.1029/2000GC000109

Minguillón, M.C., Monfort, E., Escrig, A., Celades, I., Guerra, L., Busani, G., Sterni, A., Querol, X. (2013). Air quality comparison between two European ceramic tile clusters. Atmos. Environ. 74, 311–319. https://doi.org/10.1016/j.atmosenv.2013.04.010

Minguillón, M.C., Cirach, M., Hoek, G., Brunekreef, B., Tsai, M., de Hoogh, K., Jedynska, A., Kooter, I.M., Nieuwenhuijsen, M., Querol, X. (2014). Spatial variability of trace elements and sources for improved exposure assessment in Barcelona. Atmos. Environ. 89, 268–281. https://doi.org/10.1016/j.atmosenv.2014.02.047

Moreno, T., Pérez, N., Querol, X., Amato, F., Alastuey, A., Bhatia, R., Spiro, B., Hanvey, M., Gibbons, W. (2010a). Physicochemical variations in atmospheric aerosols recorded at sea onboard the Atlantic-Mediterranean 2008 Scholar Ship cruise (Part II): Natural versus anthropogenic influences revealed by $PM_{10}$ trace element geochemistry. Atmos. Environ. 44, 2563–2576. https://doi.org/10.1016/j.atmosenv.2010.04.027

Moreno, T., Pérez, N., Querol, X., Amato, F., Alastuey, A., Bhatia, R., Spiro, B., Hanvey, M., Gibbons, W. (2010b). Physicochemical variations in atmospheric aerosols recorded at sea onboard the Atlantic–Mediterranean 2008 Scholar Ship cruise (Part II): Natural versus anthropogenic influences revealed by $PM_{10}$ trace element geochemistry. Atmos. Environ. 44, 2563–2576. https://doi.org/10.1016/j.atmosenv.2010.04.027

Morera-Gómez, Y., Elustondo, D., Lasheras, E., Alonso-Hernández, C.M., Santamaría, J.M. (2018). Chemical characterization of $PM_{10}$ samples collected simultaneously at a rural and an urban site in the Caribbean coast: Local and long-range source apportionment. Atmos. Environ. 192, 182–192. https://doi.org/10.1016/j.atmosenv.2018.08.058

Mugica, V., Ortiz, E., Molina, L., De Vizcaya-Ruiz, A., Nebot, A., Quintana, R., Aguilar, J., Alcántara, E. (2009). PM composition and source reconciliation in Mexico City. Atmos. Environ. 43, 5068–5074. https://doi.org/10.1016/j.atmosenv.2009.06.051

Murillo, J.H., Roman, S.R., Marin, J.F.R., Ramos, A.C., Jimenez, S.B., Gonzalez, B.C., Baumgardner, D.G. (2013). Chemical characterization and source apportionment of $PM_{10}$ and $PM_{2.5}$ in the

metropolitan area of Costa Rica, Central America. Atmos. Pollut. Res. 4, 181–190. https://doi.org/10.5094/APR.2013.018

Nunes, R.A.O., Alvim-Ferraz, M.C.M., Martins, F.G., Sousa, S.I.V. (2017). Assessment of shipping emissions on four ports of Portugal. Environ. Pollut. 231, 1370–1379. https://doi.org/10.1016/j.envpol.2017.08.112

Paatero, P. (1997). Least squares formulation of robust non-negative factor analysis. Chemom. Intell. Lab. Syst. 37, 23–35. https://doi.org/10.1016/S0169-7439(96)00044-5

Paatero, P., Eberly, S., Brown, S.G., Norris, G.A. (2014). Methods for estimating uncertainty in factor analytic solutions. Atmos. Meas. Tech. 7, 781–797. https://doi.org/10.5194/amt-7-781-2014

Pan, Y., Tian, S., Li, X., Sun, Y., Li, Y., Wentworth, G.R., Wang, Y. (2015). Trace elements in particulate matter from metropolitan regions of Northern China: Sources, concentrations and size distributions. Sci. Total Environ. 537, 9–22. https://doi.org/10.1016/j.scitotenv.2015.07.060

Pant, P., Harrison, R.M. (2012). Critical review of receptor modelling for particulate matter: A case study of India. Atmos. Environ. 49, 1–12. https://doi.org/10.1016/j.atmosenv.2011.11.060

Pey, J., Querol, X., Alastuey, A. (2009). Variations of levels and composition of $PM_{10}$ and $PM_{2.5}$ at an insular site in the Western Mediterranean. Atmos. Res. 94, 285–299. https://doi.org/10.1016/j.atmosres.2009.06.006

Pey, J., Alastuey, A., Querol, X., Pérez, N., Cusack, M. (2010a). A simplified approach to the indirect evaluation of the chemical composition of atmospheric aerosols from PM mass concentrations. Atmos. Environ. 44, 5112–5121. https://doi.org/10.1016/j.atmosenv.2010.09.009

Pey, J., Querol, X., Alastuey, A. (2010b). Discriminating the regional and urban contributions in the North-Western Mediterranean: PM levels and composition. Atmos. Environ. 44, 1587–1596. https://doi.org/10.1016/j.atmosenv.2010.02.005

Police, S., Sahu, S.K., Pandit, G.G. (2016). Chemical characterization of atmospheric particulate matter and their source apportionment at an emerging industrial coastal city, Visakhapatnam, India. Atmos. Pollut. Res. 7, 725–733. https://doi.org/10.1016/j.apr.2016.03.007

Police, S., Sahu, S.K., Tiwari, M., Pandit, G.G. (2018). Chemical composition and source apportionment of $PM_{2.5}$ and $PM_{2.5–10}$ in Trombay (Mumbai, India), a coastal industrial area. Particuology 37, 143–153. https://doi.org/https://doi.org/10.1016/j.partic.2017.09.006

Querol, X., Alastuey, A., Rodriguez, S., Plana, F., Ruiz, C.R., Cots, N., Massagué, G., Puig, O. (2001). $PM_{10}$ and $PM_{2.5}$ source apportionment in the Barcelona Metropolitan area, Catalonia, Spain. Atmos. Environ. 35, 6407–6419. https://doi.org/https://doi.org/10.1016/S1352-2310(01)00361-2

Querol, X., Alastuey, A., Pey, J., Cusack, M., Perez, N., Mihalopoulos, N., Theodosi, C., Gerasopoulos, E., Kubilay, N., Kocak, M. (2009). Variability in regional background aerosols within the Mediterranean. Atmos. Chem. Phys. 9, 4575–4591. https://doi.org/10.5194/acp-9-4575-2009

Ramírez, O., Sánchez de la Campa, A.M., Amato, F., Catacolí, R.A., Rojas, N.Y., de la Rosa, J. (2018). Chemical composition and source apportionment of $PM_{10}$ at an urban background site in a high–altitude Latin American megacity (Bogota, Colombia). Environ. Pollut. 233, 142–155. https://doi.org/https://doi.org/10.1016/j.envpol.2017.10.045

Reche, C., Querol, X., Alastuey, A., Viana, M., Pey, J., Moreno, T., Rodríguez, S., González, Y., Fernández-Camacho, R., De La Campa, A.M.S., De La Rosa, J., Dall'Osto, M., Prévôt, A.S.H., Hueglin, C., Harrison, R.M., Quincey, P. (2011). New considerations for PM, Black Carbon and particle number concentration for air quality monitoring across different European cities. Atmos. Chem. Phys. 11, 6207–6227. https://doi.org/10.5194/acp-11-6207-2011

Ripoll, A., Minguillón, M.C., Pey, J., Pérez, N., Querol, X., Alastuey, A. (2015). Joint analysis of continental and regional background environments in the western Mediterranean: $PM_1$ and $PM_{10}$ concentrations and composition. Environ. Pollut. 15, 17–23. https://doi.org/10.1016/j.envpol.2015.07.004

Rizzo, L.V., Artaxo, P., Karl, T., Guenther, A.B., Greenberg, J. (2010). Aerosol properties, in-canopy gradients, turbulent fluxes and VOC concentrations at a pristine forest site in Amazonia. Atmos. Environ. 44, 503–511. https://doi.org/10.1016/j.atmosenv.2009.11.002

Rodríguez-Villamizar, L.A., Rojas-Roa, N.Y., Fernández-Niño, J.A. (2019). Short-term joint effects of ambient air pollutants on emergency department visits for respiratory and circulatory diseases in Colombia, 2011–2014. Environ. Pollut. 248, 380–387. https://doi.org/10.1016/j.envpol.2019.02.028

Rolong, G.B., Romo Padilla, A., Agudelo-Castañeda, D. (2021). Aporte de $PM_{10}$ y $PM_{2.5}$ en la calidad del aire de Barranquilla por quemas en el Vía Parque Isla de Salamanca, in: Congreso Colombiano y Conferencia Internacional de Calidad de Aire y Salud Pública (CASAP), IEEE, Bogotá, pp. 0–5. https://doi.org/10.1109/CASAP54985.2021

Rolph, G., Stein, A., Stunder, B. (2017). Real-time Environmental Applications and Display sYstem: READY. Environ. Model. Softw. 95, 210–228. https://doi.org/10.1016/j.envsoft.2017.06.025

Russo, M.A., Leitão, J., Gama, C., Ferreira, J., Monteiro, A. (2018). Shipping emissions over Europe: A state-of-the-art and comparative analysis. Atmos. Environ. 177, 187–194. https://doi.org/10.1016/j.atmosenv.2018.01.025

Salvador, P., Artíñano, B., Viana, M., Alastuey, A., Querol, X. (2012). Evaluation of the changes in the Madrid metropolitan area influencing air quality: Analysis of 1999-2008 temporal trend of particulate matter. Atmos. Environ. 57, 175–185. https://doi.org/10.1016/j.atmosenv.2012.04.026

Sánchez de la Campa, A.M., de la Rosa, J.D., González-Castanedo, Y., Fernández-Camacho, R., Alastuey, A., Querol, X., Pio, C. (2010). High concentrations of heavy metals in PM from ceramic factories of Southern Spain. Atmos. Res. 96, 633–644. https://doi.org/10.1016/j.atmosres.2010.02.011

Sharma, S.K., Mandal, T.K., Saxena, M., Rashmi, Sharma, A., Datta, A., Saud, T. (2014). Variation of OC, EC, WSIC and trace metals of $PM_{10}$ in Delhi, India. J. Atmos. Solar-Terrestrial Phys. 113, 10–22. https://doi.org/10.1016/j.jastp.2014.02.008

Sharma, S.K., Mandal, T.K., Jain, S., Saraswati, Sharma, A., Saxena, M. (2016). Source Apportionment of $PM_{2.5}$ in Delhi, India Using PMF Model. Bull. Environ. Contam. Toxicol. 97, 286–293. https://doi.org/10.1007/s00128-016-1836-1

Shivani, Gadi, R., Sharma, S.K., Mandal, T.K. (2019). Seasonal variation, source apportionment and source attributed health risk of fine carbonaceous aerosols over National Capital Region, India. Chemosphere 237, 124500. https://doi.org/10.1016/j.chemosphere.2019.124500

Taghvaee, S., Sowlat, M.H., Mousavi, A., Hassanvand, M.S., Yunesian, M., Naddafi, K., Sioutas, C. (2018). Source apportionment of ambient $PM_{2.5}$ in two locations in central Tehran using the Positive Matrix Factorization (PMF) model. Sci. Total Environ. 628–629, 672–686. https://doi.org/10.1016/j.scitotenv.2018.02.096

Teixeira, E.C., Agudelo-Castañeda, D.M., Mattiuzi, C.D.P. (2015). Contribution of polycyclic aromatic hydrocarbon (PAH) sources to the urban environment: A comparison of receptor models. Sci. Total Environ. 538, 212–219. https://doi.org/10.1016/j.scitotenv.2015.07.072

U.S. Environmental Protection Agency (U.S. EPA) (1999). Sampling of Ambient Air for Suspended Particle Matter (SPM) and $PM_{10}$ Using High Volume (HV) Sampler. EPA e-CFR Title 40, Part 50, Appendix J: $PM_{10}$.

U.S. Environmental Protection Agency (U.S. EPA) (2018). Positive Matrix Factorization Model for environmental data analyses. https://www.epa.gov/air-research/positive-matrix-factorization-model-environmental-data-analyses (accessed 31 July 2018).

Viana, M, Pey, J., Querol, X., Alastuey, A., de Leeuw, F., Lükewille, A. (2014a). Natural sources of atmospheric aerosols influencing air quality across Europe. Sci. Total Environ. 472, 825–833. https://doi.org/10.1016/j.scitotenv.2013.11.140

Viana, M., Hammingh, P., Colette, A., Querol, X., Degraeuwe, B., Vlieger, I. de, van Aardenne, J. (2014b). Impact of maritime transport emissions on coastal air quality in Europe. Atmos. Environ. 90, 96–105. https://doi.org/10.1016/j.atmosenv.2014.03.046

Weinberger, R., Weiner, T., Angert, A. (2016). Isotopic signature of atmospheric phosphate emitted from coal combustion. Atmos. Environ. 136, 22–30. https://doi.org/10.1016/j.atmosenv.2016.04.006